# Temperature diurnal variations (migrating tides) in the stratosphere and lower mesosphere based on measurements from SABER on TIMED

Frank T. Huang,[1] Richard D. McPeters,[2] Pawan K. Bhartia,[2] Hans G. Mayr,[2] Stacey M. Frith,[2] James M. Russell III,[3] and Martin G. Mlynczak[4]

Received 14 December 2009; revised 5 March 2010; accepted 31 March 2010; published 28 August 2010.

[1] Derived diurnal variations of temperature (diurnal migrating tides) in the stratosphere and lower mesosphere based on satellite measurements from SABER on TIMED are presented. They complement earlier studies by us and by others that concentrated on higher altitudes. The amplitudes range from less than 1°K to a few °K, compared to those in the upper mesosphere, which can reach 20°K. They are important to the understanding of the dynamics and energetics and can be of additional value when used with previous measurements that have records spanning decades but which do not provide adequate information to estimate diurnal variations. We compare with results by others based on satellite and ground-based measurements. At low altitudes (~25–12 hPa), the comparisons are generally quite good, even for magnitudes of 1° or less. With increasing altitude, the diurnal amplitudes display asymmetry with respect to the equator on latitude versus day coordinates up to about 1 hPa (~48 km), where a transition begins, and the morphology becomes reminiscent of the first symmetric propagating mode of the migrating tide. A transition also appears in the diurnal phase gradient with respect to altitude, where the regular progression of the diurnal phase becomes significantly smaller at altitudes from about 2.8 to 0.22 hPa. The seasonal variations can show significant semiannual behavior that peak near equinox but are less obvious at lower altitudes below ~10 hPa. Interannual variations in the upper stratosphere are qualitatively consistent with those found previously at higher altitudes by us.

**Citation:** Huang, F. T., R. D. McPeters, P. K. Bhartia, H. G. Mayr, S. M. Frith, J. M. Russell III, and M. G. Mlynczak (2010), Temperature diurnal variations (migrating tides) in the stratosphere and lower mesosphere based on measurements from SABER on TIMED, *J. Geophys. Res.*, *115*, D16121, doi:10.1029/2009JD013698.

## 1. Introduction

[2] We present derived results of temperature diurnal variations over the 24 h of local solar time (LST) with focus on the stratosphere and lower mesosphere (~25–0.1 hPa or ~25–64 km), from 48°S to 48°N latitude, for several years beginning in 2002. The results are based on measurements from the Broadband Emission Radiometry (SABER) instrument [*Russell et al.*, 1999] on the Thermosphere-Ionosphere-Mesosphere-Energetics and Dynamics (TIMED) satellite. We analyze zonal means of the data, and because of the sampling properties of SABER, these variations correspond to migrating thermal tides. Details are discussed in section 2.1 (SABER data sampling and analysis). Unlike instruments on most other satellites, SABER samples measurements over the range of local times. As discussed below, although it takes 60 days to do so and the measurements are asynoptic, they provide the potential to quantitatively estimate diurnal variations of the data. SABER data are special in the breadth of their information content. They span the globe from the stratosphere into the lower thermosphere and provide information over the 24 h of local solar time since the beginning of 2002.

[3] We also compare our results with previous studies by others, some also based on SABER data and some based on other satellites and ground-based measurements, in order to provide an assessment of the quality of the analysis and of the SABER measurements themselves.

[4] As discussed below, we [*Huang et al.*, 2006a, 2006b] and others [*Zhang et al.*, 2006; *Mukhtarov et al.*, 2009; *Xu et al.*, 2007, 2009] have previously analyzed SABER temperature data, but the emphasis was on the upper mesosphere and lower thermosphere region. In the stratosphere and lower mesosphere, there have been relatively few quantitative analyses of temperature variations over the 24 h of local time, in part because the variations are relatively

[1]Goddard Earth Sciences and Technology Center, University of Maryland, Baltimore, Maryland, USA.
[2]NASA Goddard Space Flight Center, Greenbelt, Maryland, USA.
[3]Center for Atmospheric Sciences, Hampton University, Hampton, Virginia, USA.
[4]NASA Langley Research Center, Hampton, Virginia, USA.

Copyright 2010 by the American Geophysical Union.
0148-0227/10/2009JD013698

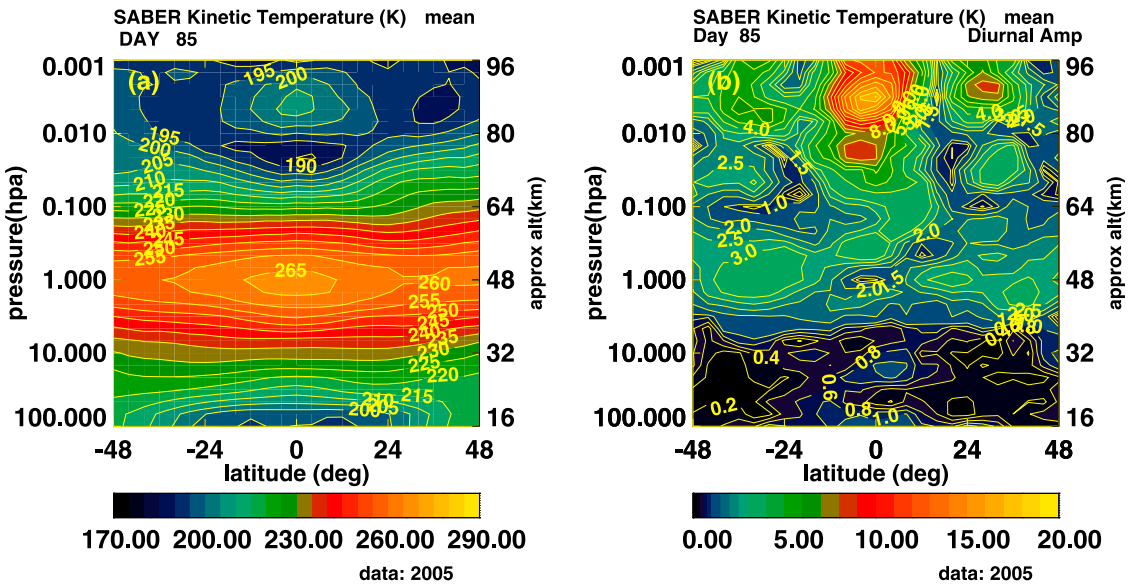


**Figure 1.** Derived zonal mean temperature (°K), based on SABER data for year 2005, on altitude (100–0.001 hPa) versus latitude (48°S–48°N) coordinates, for day 85. (a) Mean values that are averages over both local time and longitude. (b) Corresponds to Figure 1a but for diurnal amplitudes.

small and in part because few measurements provided global measurements over the range of local solar times to enable quantitative analyses. Understanding global variations of the Earth's atmospheric temperature is important for both scientific and practical reasons. The variations of temperature over a daily cycle reflect atmospheric thermal tides that result from the absorption of solar radiation and provide important information on the energetics and dynamics of the atmosphere.

[5] Derived temperature diurnal variations from SABER data can also be of value when used in conjunction with other measurements that span decades but which do not provide adequate information to estimate diurnal variations quantitatively. It can also be important in accounting for diurnal variations in estimating secular trends from various measurements [*Beig et al.*, 2003]. As an example, temperature soundings have been made over decades by the series of NOAA polar orbiters, and the long-term records are especially valuable. However, the data are nominally measured at two fixed local times only, and the orbits of some satellites have drifted so that the local times at which the measurements are made are also slowly changing. This makes calibration, continuity, and interpretation among the different data sets challenging. Understanding and having estimates of the temperature diurnal variations over 24 h in local time would potentially help to resolve these issues.

[6] To put the general morphology in perspective and context, we first present some previous results that include higher altitudes [see *Huang et al.*, 2006a, 2006b]. Figure 1a plots our derived zonal mean temperature variations on altitude-latitude coordinates from 100 to 0.001 hPa (~16–96 km) and 48°S–48°N latitude, for day of year 85, based on SABER data from 2005. Figure 1b shows the derived diurnal amplitudes corresponding to Figure 1a. It can be seen that the diurnal amplitudes are generally larger at higher altitudes and can range from less than 1°K to ~20°K. What makes Figure 1a different from most previous plots of this type, aside from the large altitude range, is that it shows our derived zonal mean values that are averages over both local time and longitude in a consistent manner. Previous results of zonal means based on other satellite data usually correspond to one local time, which can bias the values significantly. The temperature at a given local time would correspond to Figure 1a with additional variations based on the diurnal amplitudes in Figure 1b, plus higher components, superimposed.

[7] Although our focus is on the altitude range of the lower half of Figure 1 (~100–0.1 hPa), we will have occasion to compare with other results over the larger altitude range from the stratosphere into the lower thermosphere in order to assess the quality of both the measurements themselves and of the analysis we use.

## 2. Data Characteristics and Analysis

### 2.1. SABER Data Sampling and Analysis

[8] As noted earlier, SABER measurements provide the potential to estimate the variations of temperature as a function of local time over 24 h that data from other satellites generally do not provide. The SABER instrument [*Russell et al.*, 1999] views the Earth's limb to the side of the orbital plane (~74° inclination) and vertical profiles of kinetic temperature, corresponding to the line-of-sight tangent point, are retrieved from measurements of $CO_2$ 15 and 4.3 $\mu$m emissions. Here we analyze measurements made over the globe from about 31 to 0.21 hPa (~24–60 km), over 24 h in local solar time, from the beginning of 2002. The level 2A data (version 1.07), provided by the SABER project, are interpolated to 4° latitude intervals and to fixed pressure levels and, for each day, averaged over longitude for analysis.

[9] Over a given day and for a given latitude circle, measurements are made as the satellite travels northward (ascending mode) and again as the satellite travels south-

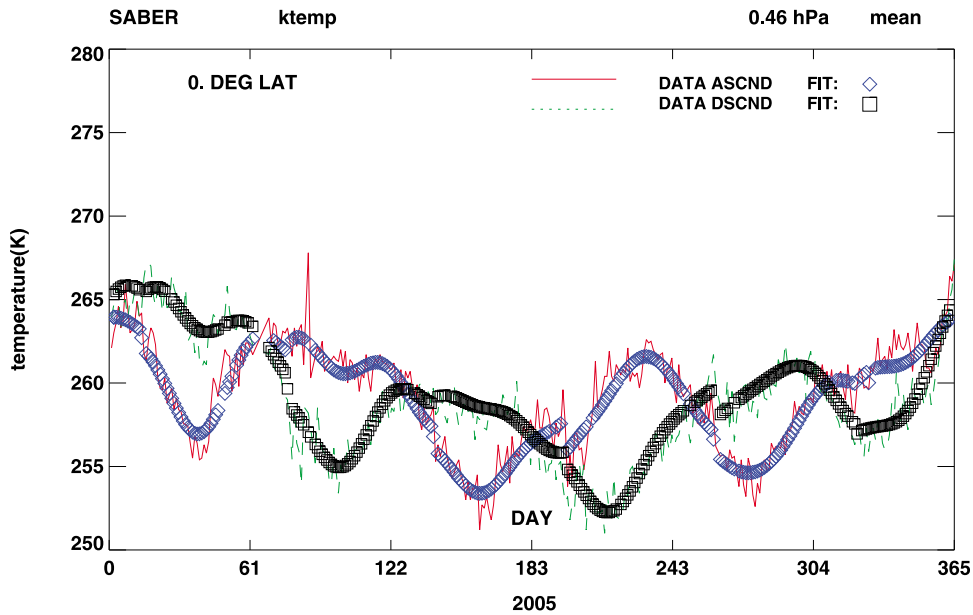


**Figure 2.** Zonally averaged SABER temperature data (°K) and estimated results plotted versus day of year for 2005, at the equator and 0.46 hPa. Solid red line and diamonds represent ascending mode data and fit, respectively. Dashed green line and squares represent descending mode data and fit, respectively.

ward (descending mode). Data at different longitudes are sampled over 1 day as the Earth rotates relative to the orbit. The orbital characteristics of the satellite are such that, over a given day for a given latitude circle and a given orbital mode (ascending or descending), the local time at which the data are measured is essentially the same, independent of longitude and time of day. For a given day, latitude, and altitude, we work with data averaged over longitude: one for the ascending orbital mode and one for the descending mode, each corresponding to a different local solar time, resulting in two data points for each day. Each can be biased by the local time variations and is therefore not a true zonal mean. True zonal means are averages made at a specific time (not over a day) over longitude around a latitude circle, with the local solar time varying by 24 h over 360° in longitude. The local times of the SABER measurements decrease by about 12 min from day to day, and it takes 60 days to sample over the 24 h of local time. Although this provides essential information over the range of local times, over 60 days, variations can be due to both local time and other variables, such as season. Diurnal and mean variations are embedded together in the data and need to be unraveled from each other to obtain more accurate estimates of each. Therefore, although SABER data provide information as a function of local time that most other satellites do not, the measurements are still asynoptic, and there may be inherent limitations to the information content.

[10] Our algorithm is designed for this type of sampling in local time and provides estimates of both diurnal and mean (e.g., annual and semiannual oscillations) variations together in a consistent manner. At a given latitude and altitude for data over a period of a year, the algorithm performs a least squares estimate of a two-dimensional Fourier series, where the independent variables are local solar time and day of year and variations as a function of local time and day of year over 1 year are generated (see Appendix A). We currently do not obtain results poleward of 48° latitude because data exist at the higher latitudes only on alternate yaw intervals (60 days). Because it takes SABER 60 days to sample over the range of local times, the sampling is less than ideal and the information of the diurnal variations may be limited to some extent, and we limit the number of coefficients estimated as described in Appendix A. Once the coefficients are estimated, both the mean components and the diurnal variations can be calculated directly for any day of year. The algorithm has been applied previously to SABER temperature and ozone measurements of diurnal variations and mean variations to study intraseasonal (ISO), semiannual (SAO), and quasi-biennial (QBO) oscillations [*Huang et al.*, 2006a, 2006b, 2008a, 2008b]. It has also been successfully applied to wind measurements from the TIMED Doppler Interferometer (TIDI), as described in th work of *Huang et al.* [2006a], and to MLS UARS ozone measurements [*Huang et al.*, 1997].

[11] Figure 2 shows an example of the sampling properties of SABER data and how well our algorithm estimates the data. We show results at the equator and 0.46 hPa (~55 km), year 2005 versus day of year, near the upper boundary of the altitude range of interest, where the diurnal variations are larger and more easily discerned graphically. For a given day, the solid red line and dashed green line represent the data averaged over longitude from the ascending and descending modes, respectively, each corresponding to one local time. As can be seen, the two data points for each day can differ significantly, reflecting different local times. The diamonds and squares depict our estimates, evaluated at the same day and same local time as the data. The estimates approximate the measurements reasonably, although we obviously cannot follow the day-to-day fluctuations and there are some intervals over several days where our estimates do not follow the data as well, so some smoothing exists.

### 2.2. SABER Data Quality and Analysis

[12] As noted earlier, we had previously presented corresponding results based on SABER temperature data in the work of *Huang et al.* [2006a, 2006b], where the focus was on higher altitudes. Also noted was the work of *Mukhtarov et al.* [2009], using the same data. They state that "the comparison between the diurnal temperatures found in this study with those by *Huang et al.* [2006b] for 2002, 2003, and 2004 indicates quite a good degree of similarity. For instance, for the equatorial March maximum at 75 km height for 2002, 2003, and 2004, we derived amplitudes of ~13°K, 9°K, and 12°K, versus those by *Huang et al.* [2006a, 2006b] of 12°K, 8°K, and 13°K, respectively. The similarity for the same maximum at 95 km height is even better; we obtained 20°K, 17°K, and 21°K versus 20°K, 17°K, and 20°K from the work of *Huang et al.* [2006a, 2006b]." This excellent agreement attests to the quality of our analysis.

[13] As for the quality of the data themselves, *Remsberg et al.* [2003] have reviewed the data quality of an earlier version of SABER temperatures. The following, taken from our results of ozone and temperature quasi-biennial oscillation correlations [*Huang et al.*, 2008a], also based on SABER measurements, should lend independent and additional support to the quality of the SABER data. As noted in the work of *Huang et al.* [2008a], systematic uncertainties in the ozone data can be relatively large, especially at higher altitudes. But for diurnal variations and quasi-biennial oscillations (QBO), which are deviations from a mean state, the uncertainties are much more reasonable. As discussed earlier, diurnal and mean variations such as the QBO are embedded together in the data and need to be unraveled from each other to obtain more accurate estimates of each. From the mathematical view, the diurnal and QBO variations in the data are on equal footing, and obtaining robust estimates for one reflects on that for the other. Our algorithm estimates these variations together. As it turns out, there is more independent corroborative evidence for the ozone and temperature QBO than for the diurnal variations, and we therefore consider the QBO for this purpose. In addition, there are expectations for the correlation between the ozone QBO and temperature QBO, which should provide further corroboration. Figure 3 shows our derived QBO results based on SABER zonal mean ozone mixing ratios (Figures 3a and 3c, ppmv) and temperatures (Figures 3b and 3d, °K), at the equator on altitude versus day coordinates, based on data from year days 2002001 to 2004060, assuming a period of 26 months, with the abscissa plotted over two cycles. The top row of Figure 3 shows the ozone QBO (Figure 3a) and the temperature QBO (Figure 3b) between 20 and 50 km. Solid contour lines denote zero and positive values, while dashed lines denote negative values. Near 28 km, the QBO ozone mixing ratios undergo relatively sharp changes in phase with altitude. Below about 28 km, the ozone and temperature are just about in phase with each other as a function of day of year. Above this altitude, the ozone and temperature are mostly out of phase. The rapid change of phase in ozone near 28 km is consistent with past observations of the QBO given by *Zawodny and McCormick* [1991], *Hasebe* [1994], and *Tian et al.* [2006] using SAGE II data and with results from the work of *Hollandsworth et al.* [1995] using SBUV data, which show a phase shift near 31 km. The stratospheric QBO has been simulated by various one-dimensional, two-dimensional, and three-dimensional models, including those of *Ling and London* [1986], *Gray and Pyle* [1989], *Hasebe* [1994], *Butchart et al.* [2003], and *Tian et al.* [2006], with attendant differences in assumptions and complexities among the models. The bottom row of Figure 3 corresponds to the top row, but for altitudes between 40 and 100 km. We have allowed the scales to saturate (near 40 km and above ~85 km) in order to show the smaller values between 45 and 85 km more clearly. It can be seen that the ozone and temperatures remain mostly out of phase with increasing altitude up to about 75 km. Between 75 and 80 km, the temperature phases change rapidly with altitude, so that above about 80 km the ozone and temperature QBOs are again more in phase with respect to day of year.

[14] The probability that the results display the generally expected phase relationships between ozone and temperature throughout the altitude range, from the stratosphere into the mesosphere and higher, is fortuitous and is extremely small. This attests to the validity of the results, both for the data and the analysis. Diurnal and mean variations such as the QBO are deviations from a mean state, and the consistency between the ozone and temperature variations throughout the different altitudes indicates that our results are robust.

[15] In addition, separate corroboration for our estimates of the temperature QBO is discussed in the work of *Huang et al.* [2006b], including comparisons with results from the U. K. Meteorological Office (UKMO) stratospheric assimilation [*Randel et al.*, 1999] and with corresponding results based on the microwave limb sounder (MLS) on the Upper Atmosphere Research Satellite (UARS).

## 3. Previous Studies

### 3.1. Empirical

[16] Previous empirical analysis of diurnal variations mostly emphasized studies at higher altitudes in the upper mesosphere and thermosphere, where tidal variations are relatively large and can dominate. We have already noted the results of tidal temperatures, also based on SABER data, by *Xu et al.* [2007, 2009], *Zhang et al.* [2006], *Mukhtarov et al.* [2009], and by us [*Huang et al.*, 2006a, 2006b]. *Wu and Jiang* [2005], *Wu et al.* [1998], and *Keckhut et al.* [1996] provided results of diurnal variations based on MLS UARS data. We have also provided some results based on MLS UARS temperature measurements [*Huang et al.*, 2006a, 2006b]. At lower altitudes, *Oberheide et al.* [2000] presented results based on satellite-borne measurements from the Cryogenic Infrared Spectrometers and Telescopes for the Atmosphere (CRISTA), and *Zeng et al.* [2008] provide results of tidal temperatures between 10 and 30 km and within 30° of the equator from the Challenging Minisatellite Payload (CHAMP) occultation observations. We will compare with both of these studies and will also have occasion to compare with ground-based lidar measurements.

### 3.2. Theoretical

[17] Theoretical studies using global models over several decades have provided essential insights to our understanding of atmospheric tides. *Chapman and Lindzen* [1970] presented a comprehensive exposition on the classical tidal

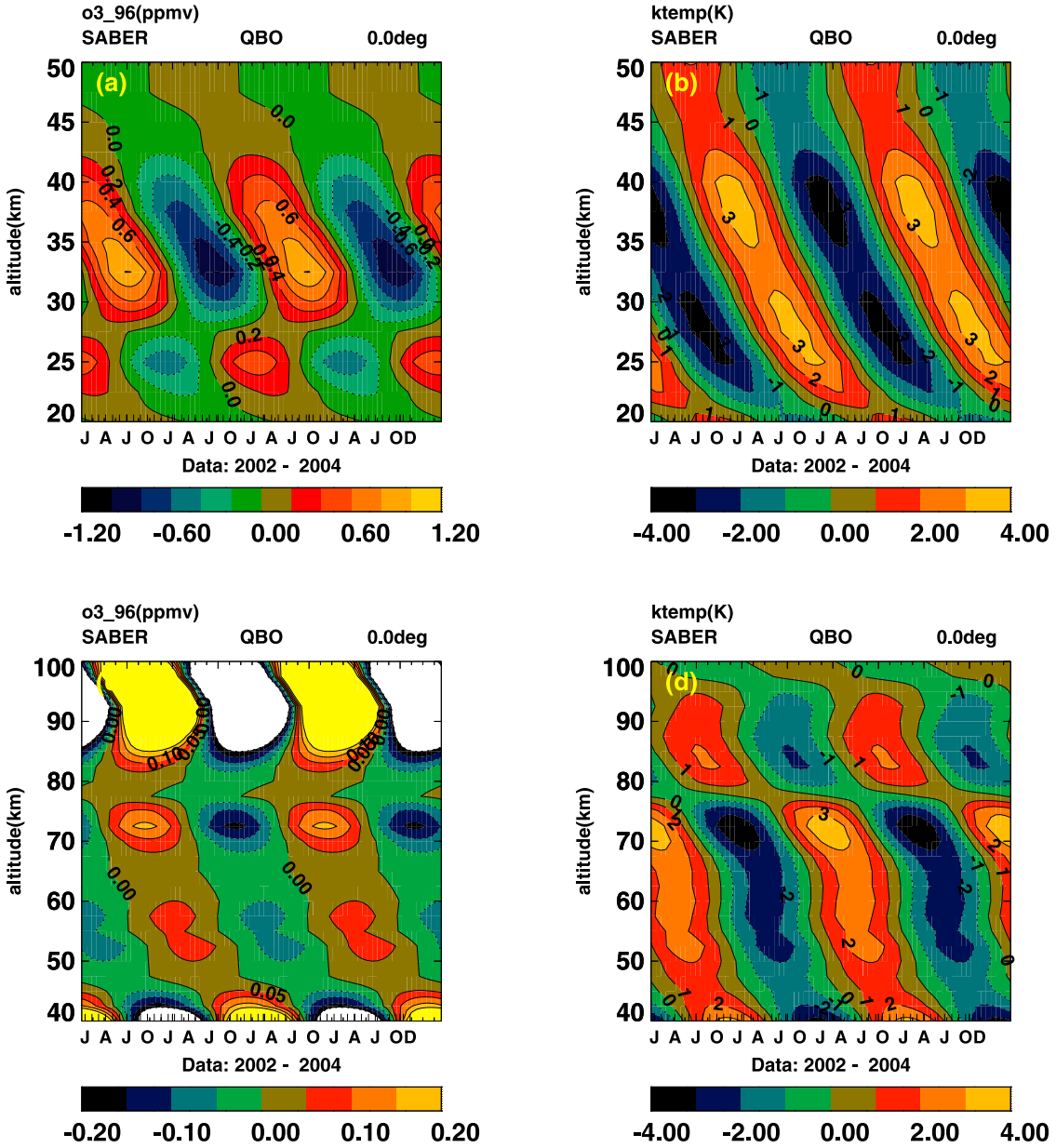


**Figure 3.** (top row) QBO results based on SABER (a) ozone (ppmv) and (b) temperatures (K) at the equator on altitude (20–50 km)-day coordinates, based on zonal mean data from year-day 2002001 to 2004060. The plots are over two cycles. Contour intervals are 0.2 ppmv for ozone and 1°K for temperature. Solid contours denote zero and positive values; dashed lines denote negative values. Below ~28 km, the ozone and temperature are mostly in phase with respect to day of year. Near 28 km, the ozone phase changes rapidly, so that above ~28 km, the ozone and temperature are mostly out of phase with respect to day of year. (lower row) Corresponds to the top row, but for altitudes between 40 and 100 km. (c) Ozone and (d) temperatures remain mostly out of phase with increasing altitude up to about 80 km. Between 75 and 80 km, the temperature changes phases rapidly with altitude, so that above about 80 km, the ozone and temperature QBO are again no longer in phase with respect to day of year.

equations and their solutions. Since then, more complex models requiring numerical solutions [e.g., *Forbes*, 1982, 1984] have further advanced our understanding to a large degree. Currently, there is a large body of research in the literature ranging from models that focus on tidal variations to general circulation models (GCM). Although great strides have been made, models of varying complexities still cannot explain all observed phenomena quantitatively. Because of the large number and variety of studies, we will only mention a few that are either associated with empirical studies or with tides, in particular. Examples include the global-scale wave model (GSWM) [*Hagan et al.*, 1999; *Hagan and Forbes*, 2003], the models of *Mayr et al.* [1998, 2005], and others, who have focused on the importance

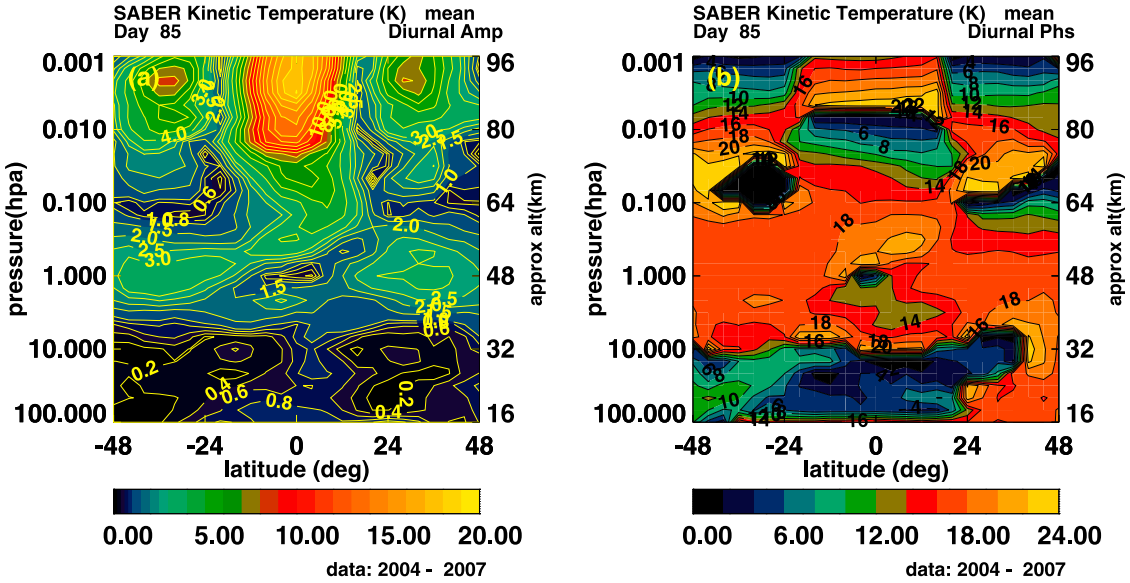


**Figure 4.** (a) Derived diurnal temperature migrating tide amplitudes on altitude (100–0.001 hPa) versus latitude (48°S–48°N) coordinates for day 85 based on SABER data from 2004 to 2007. (b) As in Figure 4a, but for diurnal phases (hour of maximum value).

of gravity waves, such as applying the Doppler spread parameterization of *Hines* [1997a, 1997b]. *McLandress* [1997] focused on tidal behavior using the Canadian middle atmosphere general circulation model (CMAM), and *Swinbank et al.* [1999] studied stratospheric tides using data assimilation in conjunction with a general circulation model (Goddard Earth Observing System, GEOS-2). These models include various forcing and dissipation mechanisms and wave-wave and wave-mean flow interactions.

## 4. Results and Comparisons

### 4.1. Diurnal Variations (Migrating Tides) With Altitude and Latitude

[18] Figure 4 shows temperature diurnal amplitudes and phases on altitude (100–0.001 hPa) versus latitude (48°S–48°N) coordinates. Figure 4a shows derived temperature diurnal migrating tide amplitudes, and Figure 4b shows the corresponding phases (hour of maximum value), for day 85, based on SABER data from 2004 to 2007. We show results at higher altitudes extending into the lower thermosphere in order to more easily make comparisons with results obtained previously by us and by others. These include results by *Zhang et al.* [2006], *Mukhtarov et al.* [2009], and *Xu et al.* [2009], which are also based on SABER measurements and presented in the form of Figure 4. However, detailed comparisons are cumbersome due to the nature of contour plots and details of contour levels. Also, the results of *Zhang et al.* [2006] are based on data from 2004 alone, while those of *Mukhtarov et al.* [2009] and *Xu et al.* [2009] are based on data from 2002 through 2007. Earlier, we had already noted that *Mukhtarov et al.* [2009] mentioned the excellent agreement between their and our results in the work of *Huang et al.* [2006b]. Our Figure 4a also compares well with Figure 3a of *Xu et al.* [2009], especially considering that their results represent the average diurnal amplitudes over 6 years, while our results in Figure 4a represent day 85 based on data from 4 years merged into one 365 day period, and the analysis techniques are not the same. In each case, the diurnal amplitudes maximize at the equator near 95 km with a value of ~16°K. *Xu et al.* [2009], *Mukhtarov et al.* [2009], and *Zhang et al.* [2006] also show another but smaller maximum near 85 km, which is not apparent in our Figure 4a. However, we do show the secondary maximum for results based on single-year data. Near ±30° latitude, *Xu et al.* [2009] and we both show local minima of ~1°K or less at ~0.1 hPa (~64 km) and local maxima of ~3°K–4°K near 1.0 hPa (~48 km).

[19] However, in these studies, the emphasis is not in the altitude range of our focus (stratosphere). *Zhang et al.* [2006] do not provide plots below 40 km, and neither *Mukhtarov et al.* [2009] nor *Xu et al.* [2009] provide detailed contours below ~45 km. For these lower altitudes, although the amplitudes are relatively small (<1°K to <3°K) as shown below in Figures 5–8, there are significant and systematic variations of interest. *Xu et al.* [2009] do provide profiles which are valuable for our discussion concerning lower altitudes in Figure 9.

[20] Of note are the diurnal phases shown in Figure 4b, where the phase progression from high altitudes changes rate near 0.1 hPa (~64 km) and on to lower altitudes. This was also noticed by *Mukhtarov et al.* [2009] in their results, and they mentioned that this change in vertical phases may be due to the superposition of trapped and propagating tidal modes and also noted that, in this region, the effect of solar radiation absorption by ozone should be dominant, giving rise to a diurnal temperature response that is affected by the trapped diurnal modes. We note also that, in the region where ozone reaches higher values, the feedback mechanisms between temperature and ozone, due in part to the dependence of chemical reactions rates on temperature [*Barnett et al.*, 1975], might also contribute to the nature of their diurnal variations. For time scales longer than 1 day, correlations between temperature and ozone are well documented.

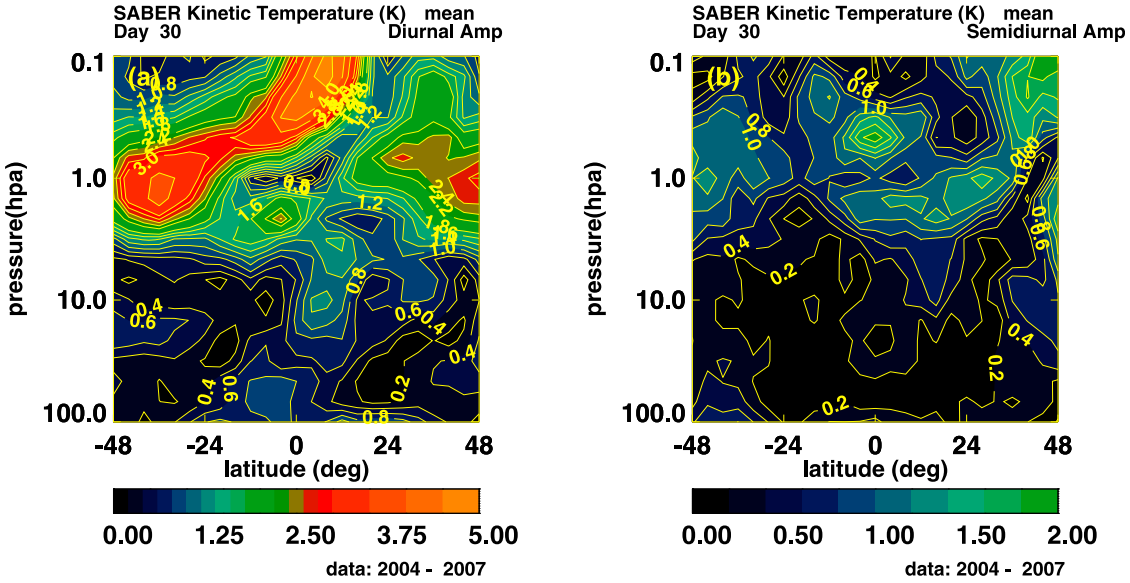


**Figure 5.** (a) Derived temperature diurnal migrating tide amplitudes. (b) Semidiurnal amplitudes, for day 30 based on SABER data from 2004 to 2007, on altitude (100–0.1 hPa) versus latitude (48°S–48°N) coordinates. It can be seen that, in the stratosphere, the diurnal amplitudes have values up to ~1°K for altitudes below about 0.68 hPa and can approach ~3°K near 1 hPa (~48 km).

More pertinent to this study are time scales less than 1 day, for which there have been few analyses. For these smaller periods, the response times of ozone and temperature to each other, in order to maintain equilibrium, has been studied by *Froidevaux et al.* [1989]. They use a daytime chemical model at midlatitudes, with input temperature perturbations of various periods, and compare the ozone response in the form of the magnitude of the correlation coefficient. They find that over a diurnal cycle, ozone and temperature variations in the upper stratosphere and lower mesosphere are expected to be correlated to varying degrees, depending on altitude, and on the trade-off between dynamics and chemistry.

[21] Figure 5 corresponds to Figure 4, but for day 30, from 100 to 0.1 hPa. The diurnal amplitudes in Figure 5a can be compared with Figure 3 in the work of *Swinbank et al.* [1999]. As noted earlier, they analyzed the data assimilation system GEOS-2 (NASA GSFC), which uses a GCM in combination with measurements. Figure 3 of *Swinbank et al.* [1999] shows an example of results from a free-running (without data assimilation) model output for January 1994. Qualitatively, the comparison with our Figure 5a, for 30 January, is generally good. We have used combined data from 2004 through 2007 to mitigate interannual differences. At the equator and ~0.46 hPa, the model results of *Swinbank et al.* [1999] appear to show values near 3.0°K, while our results show amplitudes that are only a bit larger. Near 2 hPa and midlatitudes, their largest values are ~3°K. The main difference is that, near 1 hPa in the Southern Hemisphere, their values are closer to 2.5°K. *Swinbank et al.* [1999] state that the assimilation of data (TIROS operational vertical sounder (TOVS) on NOAA polar orbiters) into the model dampens the tidal amplitudes. Among their conclusion is that the tidal variations in the TOVS data are too weak. They also state that the results from MLS UARS (derived by them) are more satisfactory, although the diurnal variation is still weaker than that in the model, especially in the Northern Hemisphere. We have also derived corresponding results from MLS UARS [*Huang et al.*, 2006a, 2006b], using the same algorithm as described here, and our MLS results are closer to those based on SABER data and to the model results.

[22] In the stratosphere, because our results based on SABER data contain diurnal variations over 24 h in local time, they provide advantages for data assimilation concerning tides. Temperature measurements from TOVS and NOAA orbiters, the most important data used by *Swinbank et al.* [1999], are made only at two local times. Our results can also be used as stand-alone sets to compare independently with models.

### 4.2. Diurnal Variations With Day and Latitude

[23] Figure 6 shows our derived temperature diurnal amplitudes plotted on latitude versus day coordinates, with each plot representing a different altitude. Here we use units of kilometers for altitude in order to directly compare with results of others. Figure 6a shows our diurnal amplitudes at 25 km (~25 hPa) based on SABER data from 2004 through 2007 merged into one 365 day period. Figure 6b corresponds to Figure 6a but at 30 km (~12 hPa), as do Figure 6c but at 42.5 km (~2 hPa), and Figure 6d but at 85 km (~0.0035 hPa), and based on data from 2004 alone. The data from different years are used to better correspond with other results, with which we compare. We first note that at 85 km (Figure 6d) the amplitudes are mostly symmetric with respect to the equator, are largest near the equator with smaller maxima at midlatitudes, and resemble the familiar first propagating symmetric mode of the migrating tide. This symmetry with respect to the equator at 85 km is no longer apparent at the lower altitudes in Figures 4b and 4c, representing 30.0 and 42.5 km, respectively. With increasing altitude, at ~48 km (~1 hPa, not shown), the symmetry is again apparent, where the amplitudes at low latitudes are

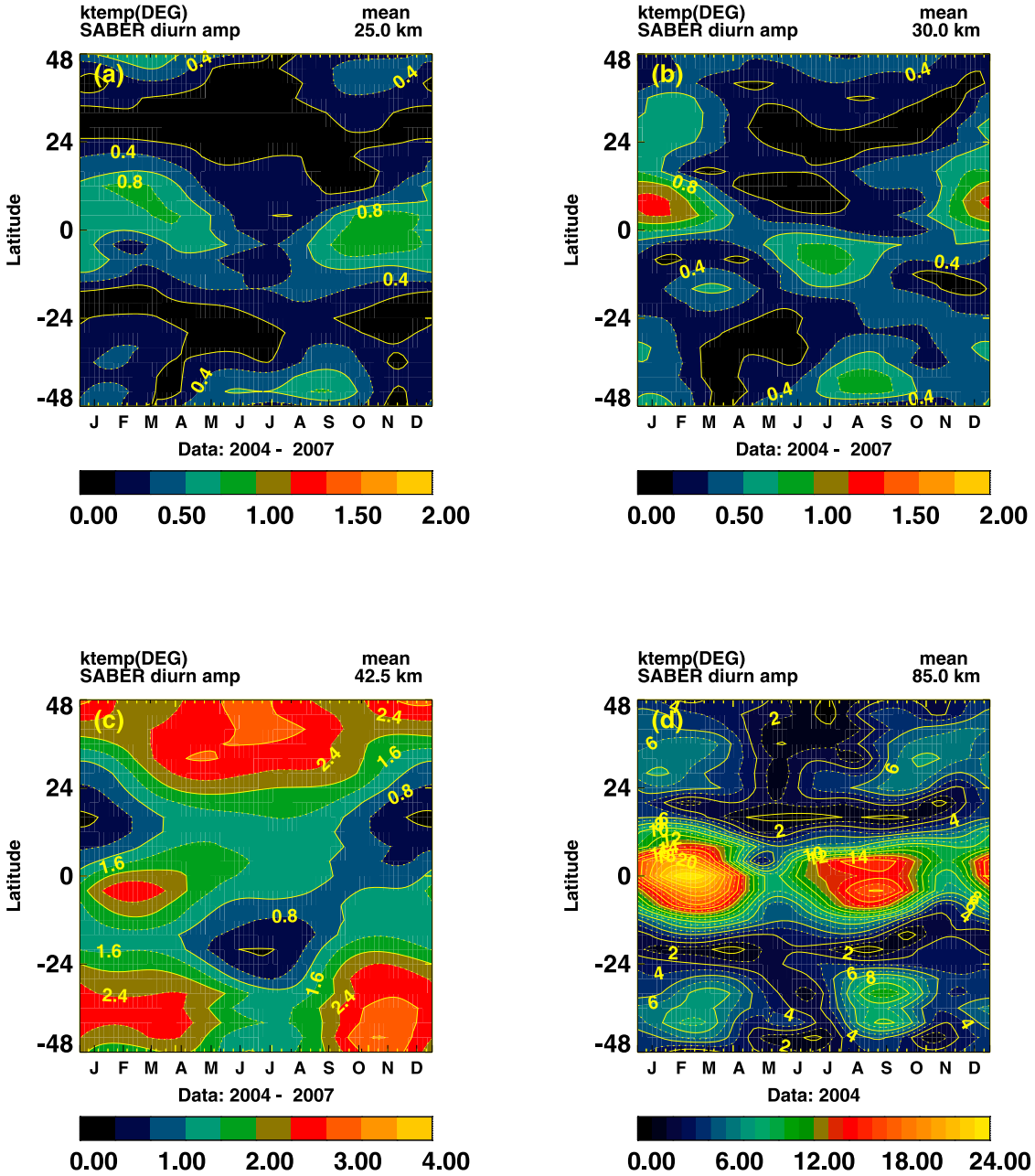


**Figure 6.** Derived diurnal migrating tide amplitudes on latitude versus day coordinates. (a) At 25 km, based on data from 2004 to 2007; contour interval is 0.2°K. (b) As in Figure 6a, but for 30 km; contour interval is 0.2°K. (c) As in Figure 6a, but at 42.5 km; contour interval is 0.4°K. (d) As in Figure 6a, but at 85 km, based on data from 2004; contour interval is 1°K.

significantly smaller than those at midlatitudes (less than 1°K versus 3°K–4°K). At the higher altitudes where there is mostly symmetry relative to the equator, the diurnal amplitudes show a semiannual variation that peaks near solstice, beginning ~0.46 hPa (55 km). Figure 6d at 85 km can be compared with corresponding results from the works of *Zhang et al.* [2006] and *Mukhtarov et al.* [2009], both also based on SABER data. At 85 km, although the relative morphologies compare very well, our diurnal amplitudes are mostly somewhat larger than those obtained by *Zhang et al.* [2006]. As mentioned earlier in section 2, our diurnal amplitudes at 75 and 95 km, noted by *Mukhtarov et al.* [2009], are virtually the same as theirs.

[24] Figure 6b, for 30 km, can be compared with those of *Zeng et al.* [2008], who have derived diurnal amplitudes and phases based on limb viewing radio occultation, using radio signals transmitted by the global positioning system (GPS) satellites. Retrieved temperatures between 10 and 30 km and within 30° latitude of the equator from the Challenging Minisatellite Payload (CHAMP) occultation observations during May 2001 to August 2005 were analyzed to derive the diurnal amplitudes and phases. They state that the retrieved temperature in the upper mesosphere lower stratosphere is

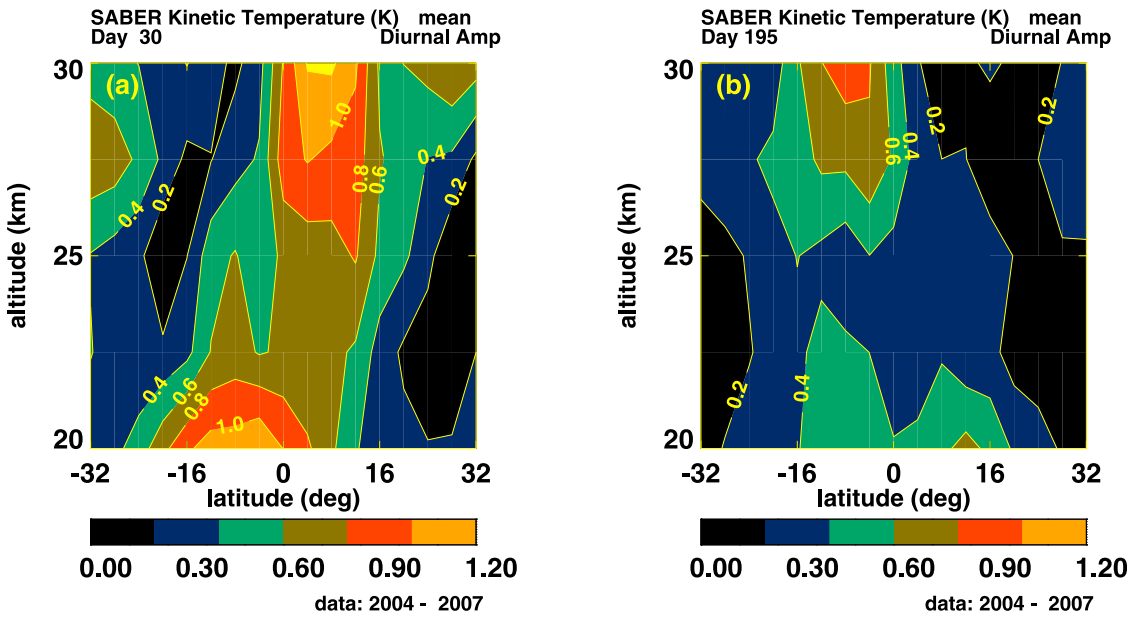


**Figure 7.** Derived migrating tide diurnal amplitudes on altitude (20–30 km) versus latitude (32°S–32°N) coordinates for days (a) 30 and (b) 195, based on SABER data from 2004 through 2007. Contour interval is 0.2°K.

accurate to within 1°K–2°K. Comparison of our Figure 6b with Figure 8a (not shown here) of *Zeng et al.* [2008] is very good, where they provide a similar plot at 30 km, within 30° of the equator versus day of year. We both show a high between 0° and 10°N latitude between about October and March, with maximums occurring early in the year. Our maximum approaches ~1.2°K compared to ~1.0°K obtained by *Zeng et al.* [2008]. We both also see another high between 0° and ~15°S latitude near the summer months, with our maximum approaching ~1°K amplitude, while that obtained by *Zeng et al.* [2008] appears to be also ~1°K or a bit larger. So at low latitudes, the diurnal amplitudes show more of an annual cycle, but variations are out of phase between the Northern and Southern hemispheres. As also shown in the work of *Zeng et al.* [2008], corresponding results from the Canadian Middle Atmosphere General Circulation Model (CMAM) [e.g., *McLandress*, 1997] also show similar variations, although there are delays in phase of a month or two and the amplitudes are higher by about 50%. At other areas, we both see smaller amplitudes mostly of 0.5°K or less. Compared to *Zeng et al.* [2008], we appear to show more structure as evidenced by the various local maxima (e.g., at 16°S and March). Differences are expected since our data are from different years. Also day of year is an independent variable in our Fourier estimate. It is not clear exactly how *Zeng et al.* [2008] represent their variations.

[25] Aside from the symmetry of the morphology of the diurnal tide with respect to the equator, there is also an asymmetry in the magnitude of the tides with respect to the equator. The asymmetry with respect to the equator shown in Figure 6 was also obtained by *Zhang et al.* [2006] at altitudes between 40 and 60 km. Because of this, they state that a reexamination of stratospheric tidal heating in their model, as well as a more comprehensive look at the measured (SABER) temperature response and its consistency with other observational data is warranted. Although we also see an asymmetry in amplitude, it is less pronounced. However, the agreement of our results at 30 km with those of *Zeng et al.* [2008] including the asymmetry, as well as the consistency with the CMAM noted by *Zeng et al.* [2008], supports the quality of the SABER measurements. *Zeng et al.* [2008] do not give results above 30 km, and *Zhang et al.* [2006] do not provide results below 40 km.

[26] Figure 7 shows our results of migrating tide diurnal amplitudes on altitude (20–30 km) versus latitude (32°S–32°N) coordinates for days 30 (Figure 7a) and 195 (Figure 7b), based on SABER data from 2004 through 2007. This is shown again to compare directly with results of *Zeng et al.* [2008, Figure 7] (December–January–February and June–July–August plots). The data used by *Zeng et al.* [2008] are discussed in relation to Figure 6. The local maximum near 30 km and ~8°N latitude in Figure 7a extends downward to lower altitudes and compares well with the results of *Zeng et al.* [2008], even for diurnal temperature amplitudes of ~0.5°K to ~1.0°K. The maximum obtained by *Zeng et al.* [2008] appears to be somewhat closer to the equator but is otherwise consistent with our results for 25 km in Figure 6a. The local maximum near 30 km and ~8°S in Figure 7b also compares well with the results of *Zeng et al.* [2008], even for temperature amplitudes of ~0.5°K to ~1.0°K. The details of the differences begin to diverge at lower altitudes below 25 km.

### 4.3. Interannual Variations

[27] Figure 8 shows diurnal amplitudes at the equator, on altitude (100–0.1 hPa, ~16–64 km) versus day of year coordinates, for years 2002 (Figure 8a), 2003, 2004, and 2005 (Figure 8d), respectively. It appears that above ~10 hPa, the magnitudes are larger for years 2002 and 2004 compared to 2003 and 2005. This is qualitatively consistent with

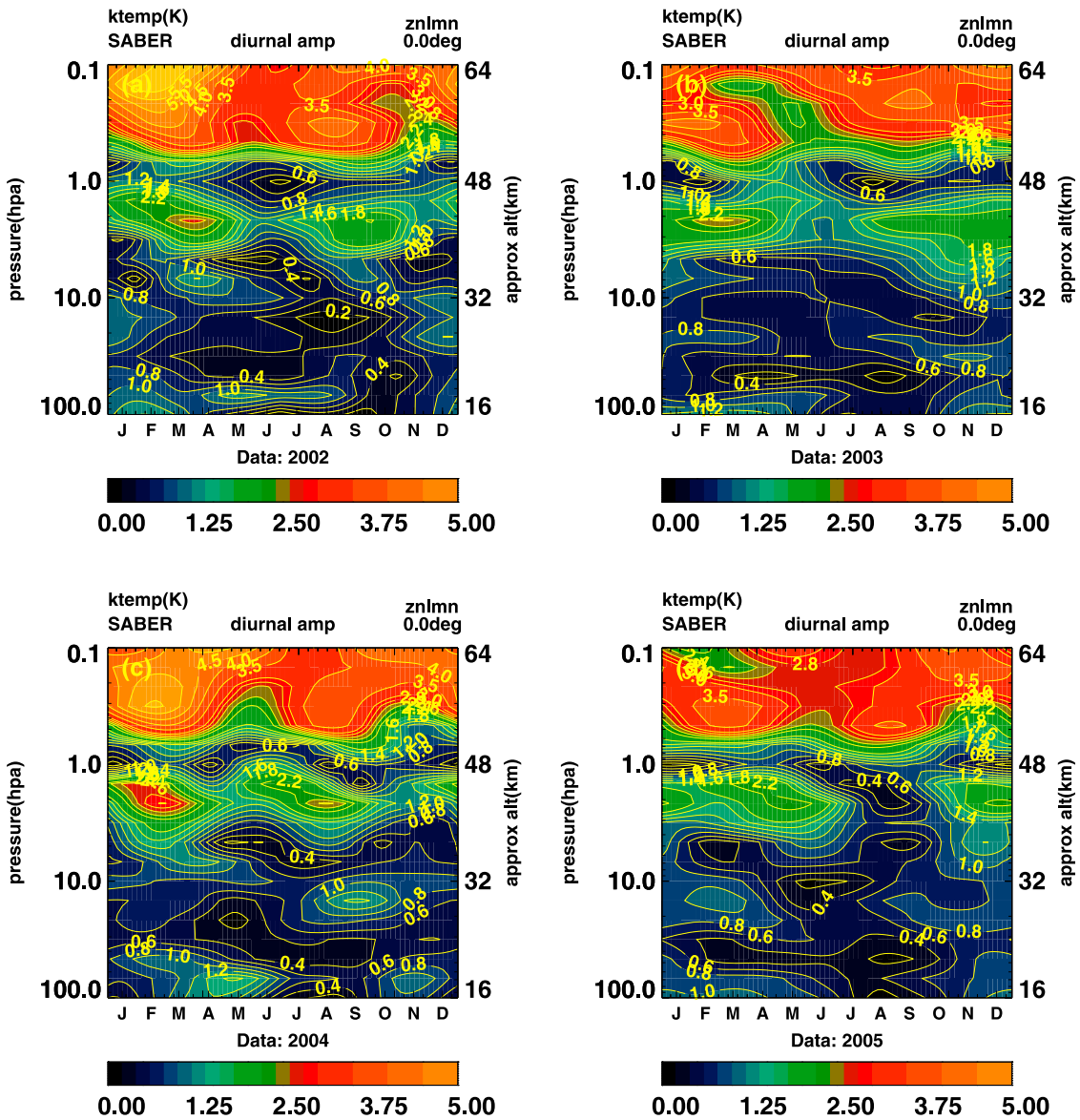


**Figure 8.** Temperature migrating tide diurnal amplitudes at the equator, on altitude (100–0.1 hPa, ~16–64 km) versus day-of-year coordinates: (a) 2002, (b) 2003, (c) 2004, and (d) 2005. Evident are interannual variations near 2.1 hPa, where the amplitudes are largest in 2004 compared to other years.

corresponding interannual variations at higher altitudes. *Huang et al.* [2006b] show that, at 75 km, the equatorial maxima of the diurnal amplitude are ~12°K for spring 2002, ~8°K for autumn 2002, spring 2003, and autumn 2003, respectively, and recover to ~12°K for 2004. We noted, as has *Mukhtarov et al.* [2009], *Xu et al.* [2009], and *Mayr and Mengel* [2005], the possibility of effects related to the QBO. Although further analysis is outside the scope of this paper, we note that SABER has been making near continuous measurements since the beginning of 2002 and provides valuable information for a further and detailed analysis.

[28] Also consistent with results at higher altitudes are the semiannual nature of the variations. In addition, they qualitatively agree with corresponding results derived by us, using the same algorithm on data from the microwave limb sounder (MLS) on the upper atmosphere research satellite (UARS; not shown). Examples are the evident semiannual behavior near 2.1 hPa and similar but smaller variations near 100 hPa.

### 4.4. Additional Comparisons

[29] At the equator, our diurnal amplitudes can also be compared with those by *Oberheide et al.* [2000], who presented results based on measurements from the Cryogenic Infrared Spectrometers and Telescopes for the Atmosphere (CRISTA), taken from 5–11 November 1994, together with corresponding results from the global-scale wave model (GSWM) [*Hagan et al.*, 1999]. The shortness of the mission (the instrument was flown on the space shuttle mission STS 66) prevented measurements over an adequate range of local times to estimate diurnal variations globally. However, near the equator, *Oberheide et al.* [2000] state that they were able

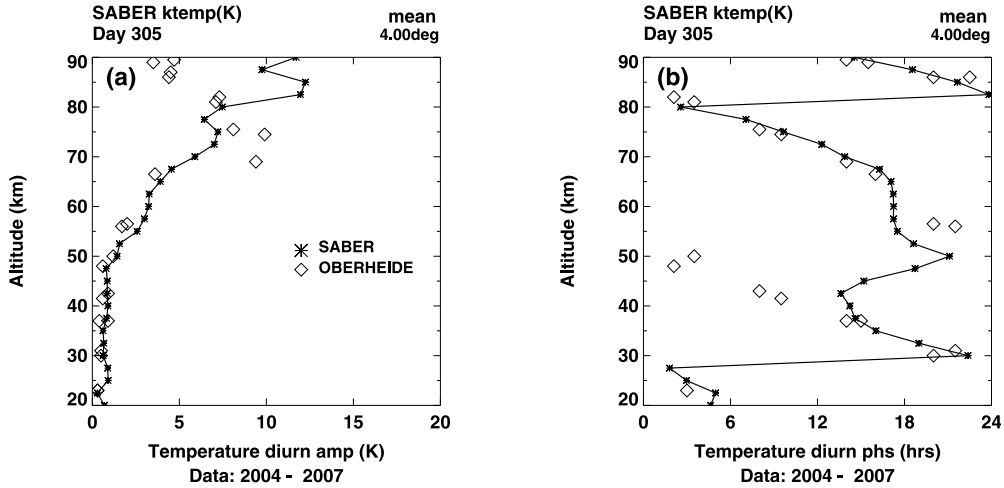


**Figure 9.** (a) Temperature diurnal amplitudes (°K) versus altitude (20–90 km) at 4°N latitude. (b) Corresponds to Figure 9a, but for phases (hour of maximum value). Asterisks denote our results based on SABER data, and diamonds denote results of *Oberheide et al.* [2000] based on CRISTA measurements.

to estimate diurnal amplitudes and phases from measurements at the ascending and descending modes, since the local times were 12 h apart.

[30] In Figure 9, the diamonds denote the results of *Oberheide et al.* [2000] that we manually transcribed from their Figure 11, representing days 5 and 9 November 1994, based on measurements between 0° and 10°N latitude, and the asterisks represent our results for day 305 based on SABER data from 2004 to 2007 merged together to mitigate differences in interannual variations. Figures 9a and 9b show diurnal amplitudes (°K) and phases (hour of maximum value), respectively, as a function of altitude (km). It can be seen that, up to about 65 km, the amplitudes agree very well, while the *Oberheide et al.* [2000] amplitudes diverge from ours near 70 km and above. Although not shown here, *Oberheide et al.* [2000] also shows results from the GSWM model [*Hagan et al.*, 1999] that was "tuned," using input ambient parameters consistent with CRISTA flight conditions such as temperature, ozone, and pressure. Although not shown here, results from the revised GSWM are also plotted in Figure 11 of *Oberheide et al.* [2000], and the amplitudes agrees very well with those of *Oberheide et al.* [2000], except above 75 km, where the model results are more consistent with our amplitudes, with both continuing to increase above 75 km, while those of *Oberheide et al.* [2000] begin to decrease. At 90 km, the GSWM diurnal amplitude is ~11°K, while those of *Oberheide et al.* [2000] is ~4°K, and our amplitude at 90 km is ~12°K. Our and the GSWM amplitudes appear to be more consistent (from their contour plots) with those of *Zhang et al.* [2006], also based on SABER data. Diurnal phases from *Oberheide et al.* [2000] are in excellent agreement with those of GSWM throughout. As can be seen from Figure 9b, our phases also agree with those of *Oberheide et al.* [2000] from 65 to 90 km. Near 65 km, our phases show a marked inflection while those of Oberheide show a less extreme inflection (as does the GSWM). Between 20 and 35 km, our phases again agree very well. The differences are in the altitude interval 35–60 km, where our results show another inflection near 40–45 km, while those of Oberhdeide show a mild inflection between ~30 and 38 km. However, the profiles in Figures 5a and 6a of *Xu et al.* [2009], also based on SABER data, agree well with our results in Figure 9 over the whole altitude range, so the differences between our results and those of *Oberheide et al.* [2000] are not due to our analysis. We also do not believe that the difference in the phases between ~40 and 60 km is due the quality of the SABER data, as discussed in relation to Figure 3, which show that the expected temperature and ozone QBO are as expected over the entire altitude range. In addition, *Haefele et al.* [2008] show diurnal temperature variations from a variety of sources, both measurements and models, at 45 km (their Figure 4), and generally the hour of maximum appears to be near 19 h local time, more consistent with our results. We had mentioned earlier that *Mukhtarov et al.* [2009] suggested that the reason the different phase structure at these levels could be due to the superposition of propagating and trapped tidal modes below 70 km. We also noted that in the lower mesosphere and stratosphere where ozone reaches higher values, the feedback mechanisms between temperature and ozone, due in part to the dependence of chemical reaction rates on temperature (see discussion for Figure 4, section 4.1), can also contribute to their diurnal variations.

[31] We also compare with ground-based lidar measurements. Figure 10 plots our diurnal amplitudes and phases (asterisks) together with the lidar results of *Gille et al.* [1991] (plus) and model results of *Forbes and Gillette* [1982] (squares). Both the lidar and model results were manually transcribed by us from the work of *Gille et al.* [1991]. The diurnal amplitudes and phases of *Gille et al.* [1991] were derived from lidar measurements made in France, at 44°N, 6°E latitude, from 30 to 80 km in altitude, made in two 11 day series of data, from November 1988 and January 1989. The top row of Figure 10 plots our diurnal amplitudes (Figure 10a) and phases (Figure 10b) for day 320 to correspond to November based on SABER data from 2004 through 2007. The bottom row of Figure 10 corresponds to the top row, but for day 30, to represent January. Although *Gille et al.* [1991] provide results up to 80 km, they caution that diurnal amplitudes and phases above 60 km have very

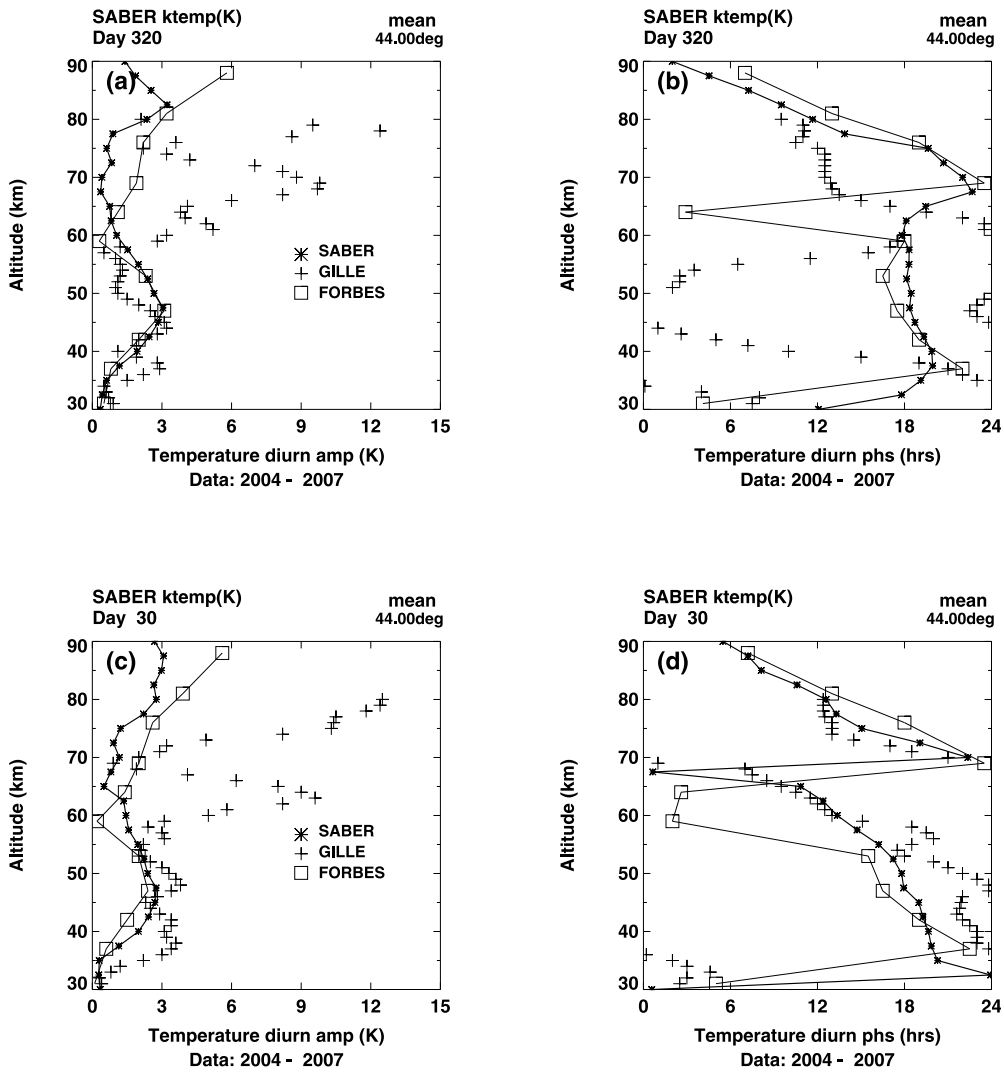


**Figure 10.** Diurnal amplitudes (°K) and phases (hour of maximum value) at 44°N latitude, based on SABER data (asterisks), *Gille et al.* [1991] amplitudes based on lidar data (plus), and model of *Forbes and Gillette* [1982] (diamonds), as a function of altitude. (a) Amplitudes corresponding to day 320 based on SABER data (from 2004 through 2007). Pluses denote lidar data taken in January, 1989, and squares denote model results from the model of *Forbes and Gillette* [1982]. (b) Corresponds to Figure 10a, but for phases. (c and d) Corresponds to Figures 10a and 10b, but for day 30. Lidar data taken in November 1989.

large uncertainties, as measurements cannot be taken over much of the daylight hours. As can be seen in Figure 10, our amplitudes agree reasonably up to ~60 km. A curious property is that our phases agree more with those of the model [*Forbes and Gillette*, 1982] compared to those of *Gille et al.* [1991]. Although not shown, we have also compared with results derived from lidar measurements by *Leblanc et al.* [1999a, 1999b] and *Yuan et al.* [2006]. There, they compared with the more recent GSWM model [*Hagan et al.*, 1999], and again our phases were much more consistent with those of the GSWM than those derived from lidar data by *Leblanc et al.* [1999a, 1999b]. Some of the differences can be explained in that we analyze zonal averages, resulting in migrating tides, while lidar measurements are all made at specific longitudes and can also reflect variations due to other types of waves. Also, the lidar measurements only represent nighttime data over a period 10 h, and *Leblanc et al.* [1999a, 1999b] estimated diurnal and semidiurnal amplitudes from these data alone.

[32] *Wu and Jiang* [2005] present results based on a late version (to extend to higher altitudes) of MLS UARS measurements within 20° of the equator from 46.42 hPa (~22 km) to 0.01 hPa (~80 km) from October 1991 to April 1993. Like SABER, MLS on UARS also samples over the range of local times and provides continuous measurements within 32° of the equator (it is not clear why the results stop at 20° latitude). *Wu and Jiang* [2005] find that, near the stratopause, the tidal amplitudes reach a maximum near March with a somewhat smaller maximum near September, which is qualitatively consistent with our results. They also state that their QBO and SAO variations exhibit "good coherency" at higher altitudes. However, it is difficult to

compare details more quantitatively with their contour plots. Our diurnal amplitudes appear to be of the same order of magnitude as those of *Wu et al.* [1998] at lower altitudes, but their diurnal amplitudes appear to be significantly smaller than ours at higher altitudes. For example, at the equator and 0.01 hPa, our diurnal amplitudes are about twice as large (~8°K versus ~4°K). We note that we and *Wu et al.* [1998] use different algorithms.

## 5. Summary and Discussion

[33] We have derived results of temperature migrating tides, based on SABER measurements, with focus in the stratosphere and lower mesosphere, within 48° of the equator, over several years, beginning in 2002. The diurnal amplitudes in this altitude range from less than 1°K to several °K. This complements our earlier works, which concentrated on higher altitudes in the mesosphere and lower thermosphere and where the diurnal amplitudes can reach 20°K or more. To help assess the quality of the results, we have compared our results with those by others, some also based on SABER data, some based on other satellite-borne instruments, and some from ground-based measurements. Generally, the comparisons support the quality of both the SABER data and the analysis. The comparisons are extended to higher altitudes in the interest of presenting a more complete picture. For example, at 85 km (cf. Figure 6d), the results reflect the familiar first symmetric propagating mode, in good agreement with corresponding results by *Mukhtarov et al.* [2009] and *Zhang et al.* [2006], also based on SABER data, but using different analyses algorithms. The agreement also continues to lower altitudes, although *Mukhtarov et al.* [2009] and *Zhang et al.* [2006] concentrate more on the higher altitudes. This attests to the quality of our analysis technique, although not to the quality of data itself.

[34] As for the quality of the SABER data, our results at 25 and 30 km (cf. Figures 6a, 6b and 7a, 7b) compare very well with those of *Zeng et al.* [2008] based on satellite measurements from CHAMP. The corresponding morphologies (in latitude-day and latitude-altitude coordinates) are consistent even for diurnal amplitudes of ~1°K or less.

[35] As the altitude increases from 25 km, the symmetry of the diurnal amplitudes with respect to the equator also seen at 85 km is not apparent at 30.0 and 42.5 km, respectively. Rather, the structure is more antisymmetric with respect to the equator. Near 50 km, the symmetry is again apparent, but the amplitudes at low latitudes are smaller than those at midlatitudes. Comparisons with results based on data from CHAMP [*Zeng et al.*, 2008] at 30 km also support this asymmetry as well. *Zeng et al.* [2008] do not provide results above 30 km.

[36] In the upper stratosphere and lower mesosphere, we find that the rate of the diurnal phase progression as a function of altitude becomes significantly smaller than that at higher altitudes (above ~64 km or 0.1 hPa), which are also found by *Mukhtarov et al.* [2009] and *Zhang et al.* [2006]. They note that in this region, the effect of solar radiation absorption by ozone should be dominant, giving rise to a diurnal temperature response that is affected by the trapped diurnal modes. It should also be noted that, in this region, where ozone values are relatively large, the feedback mechanisms between temperature and ozone, due in part to the effect of temperature on chemical reaction rates, might also contribute to the nature of their diurnal variations. This change in the vertical phase gradient of the diurnal component is not consistent with results based on CRISTA (see discussion of Figure 9) measurements near the equator. In our altitudes of interest, the diurnal amplitudes compare very well, but our phases between ~40 and 60 km (~2.8–0.2 hPa) are significantly different from those based on CRISTA data. However, *Haefele et al.* [2008] show diurnal temperature variations from a variety of sources, both measurements and models, at 45 km (their Figure 4), and generally the maximum values appear to be near 19 h, more consistent with our results. We have shown that our results at lower and higher altitudes than this are supported by independent results related to both the analysis and the quality of the data, so it is unlikely that our results are spurious only in this altitude interval. In addition, we have given evidence (see discussion to Figure 3, section 2.2) that the SABER temperature and ozone data are robust over the whole altitude range, based on our earlier analysis of correlations between temperature and ozone quasi-biennial oscillations [*Huang et al.*, 2008a].

[37] We have also presented diurnal amplitudes for different years at the equator. Above 10 hPa, they are qualitatively consistent with corresponding interannual variations at higher altitudes, where the magnitudes are larger for years 2002 and 2004 compared to those for 2003 and 2005. These interannual variations are possibly related to effects of the QBO and a detailed analysis of the SABER data, now spanning the years from 2002, may provide definitive information.

[38] Our results can be of value when used in conjunction with other measurements that have longer records spanning decades but which do not provide adequate information to estimate diurnal variations. It can also be important to account for diurnal variations in estimating secular trends from measurements [*Beig et al.*, 2003]. As an example, temperature soundings have been made over decades by the series of NOAA polar orbiters, and the long-term records are especially valuable. However, the data are nominally measured at fixed local times, and the orbits of some satellites have drifted so that the local times at which the measurements are made are also slowly changing, making calibration, continuity, and interpretation among the different data sets problematical. Understanding and having estimates of the temperature diurnal variations over 24 h in local time would potentially help to resolve these issues.

## Appendix A: Data Analysis Algorithm

[39] For a given latitude and altitude, the algorithm performs a two-dimensional Fourier least squares analysis in the form

$$\Psi(t_1, d, z, \theta, \lambda) = \sum_n \sum_k b_{nk}(z, \theta, \lambda) e^{i2\pi n t_1} e^{i2\pi k d/N}, \qquad \text{(A1)}$$

where $\Psi(t_1, d, z, \theta, \lambda)$ represents the input data: $z$ is altitude, $d$ is day of year, $\theta$ is latitude, $\lambda$ is longitude (radians), $t_1$ = local solar time (fraction of a day) = $t + \lambda/2\pi$, $t$ = time of day (fraction of day), and $N$ is the number of days in the fun-

damental period. For example, if we analyze data over 1 year, then $N = 365$.

[40] In this study, we apply the algorithm to data averaged over longitude, although it has been applied to data with longitude variations as well [*Huang and Reber*, 2004]. For cases where we wish to analyze variations with longitude as well, we use data at discrete longitudes $\{\lambda_i\}$ to find the set $b_{nk}$ $(z, \theta, \lambda_i)$ from (A1). To analyze the behavior with longitude, we estimate $\alpha_{mnk}$ $(z, \theta)$ from

$$b_{nk}(z, \theta, \lambda_i) = \sum_m \alpha_{mnk}(z, \theta) e^{i2\pi m\lambda_i/2\pi}, \qquad \text{(A2)}$$

again using a least squares fit. Finally, for any day of year $d_0$, we can sum (A1) over $k$ to obtain

$$\Psi(t, d_0, z, \theta, \lambda) = \sum_m \sum_n \beta_{nm}(z, \theta) e^{i2\pi m\lambda/2\pi} e^{i2\pi nt}, \qquad \text{(A3)}$$

where we use $\beta_{nm}$ to denote the transform to universal time $t$ (fraction of a day).

[41] If we average the data over longitude, then we obtain the migrating diurnal variations and mean flows [*Huang and Reber*, 2004] from (A1), where the coefficients are no longer dependent on $\lambda$. Once we have estimated the coefficients in (A1) or (A3), we can directly generate the diurnal variations for composition, winds, and temperature as a function of day of year, longitude, and time. TIMED sampling patterns are such that data at latitudes poleward of about 50° are made only for alternate yaw periods. Therefore, our current analyses are made only within 48° of the equator.

[42] Our fits to the data are based on data over a period of 1 year or more. Currently in (A1), the maximum value of $n$ is 5 for ozone, and the maximum of $k$ depends on the fundamental period in day of year. Because it takes SABER 60 days to sample over the range of local times, when the fundamental day-of-year period is 365 days, we estimate the coefficients $b_{nk}$ $(z, \theta, \lambda_i)$ for $k$ greater than or equal to 3 only for $n = 0$, and the maximum of $k$ is 6. When the fundamental period corresponds to the QBO, the number of terms for day of year is scaled up accordingly. The current version of the data does not provide for uncertainties, and we also assume that the uncertainties of the data are proportional to the data values themselves.

[43] **Acknowledgments.** We thank the Editor, Joost de Gouw, and three reviewers for insightful comments that helped to improve the manuscript. Funding for FTH was by the Goddard Earth Sciences and Technology Center (GEST) and NASA.

## References

Barnett, J. J., J. T. Houghton, and A. J. Pyle (1975), Temperature dependence of the ozone concentration near the stratopause, *Q. J. R. Meteorol. Soc.*, *101*, 245.

Beig, G., et al. (2003), Review of mesospheric temperature trends, *Rev. Geophys.*, *41*(4), 1015, doi:10.1029/2002RG000121.

Butchart, N., A. A. Scaife, J. Austin, S. H. E. Hare, and J. R. Knight (2003), Quasi-biennial oscillation in ozone in a coupled chemistry climate model, *J. Geophys. Res.*, *108*(D15), 4486, doi:10.1029/2002JD003004.

Chapman, S., and R. S. Lindzen (1970), *Atmospheric Tides*, Springer, New York Hines, CO.

Forbes, J. M. (1982), Atmospheric tides: 1. Model description and results for the solar diurnal component, *J. Geophys. Res.*, *87*, 5222–5240.

Forbes, J. M. (1984), Middle atmosphere tides, *J. Atmos. Terr. Phys.*, *46*, 1049–1067.

Forbes, J. M., and D. F. Gillette (1982), A compendium of theoretical atmospheric tidal structures, AFGL tech. rep., AFGL-TR-82-0173(I).

Froidevaux, L., M. Allen, S. Berman, and A. Daughton (1989), The mean ozone profile and its temperature sensitivity in the upper stratosphere and lower mesosphere: An analysis of LIMS observations, *J. Geophys. Res.*, *94*, 6389–6417.

Gille, S. T., A. Hauchecorne, and M.-L. Chanin (1991), Semidiurnal and diurnal tidal effects in the middle atmosphere as seen by Rayleigh lidar, *J. Geophys. Res.*, *96*, 7579–7587.

Gray, L. J., and J. A. Pyle (1989), A two-dimensional model of the quasi-biennial oscillation of ozone, *J. Atmos. Sci.*, *46*, 203–220.

Haefele, A., K. Hocke, N. Kampfer, P. Keckhut, M. Marchand, S. Bekki, B. Morel, T. Egorova, and E. Rozanov (2008), Diurnal changes in middle atmospheric H2O and O3: Observations in the Alpine region and climate models, *J. Geophys. Res.*, *113*, D17303, doi:10.1029/2008JD009892.

Hagan, M. E., and J. M. Forbes (2003), Migrating and nonmigrating semidiurnal tides in the middle and upper atmosphere excited by tropospheric latent heat release, *J. Geophys. Res.*, *108*(A2), 1062, doi:10.1029/2002JA009466.

Hagan, M. E., M. D. Burrage, J. M. Forbes, J. Hackney, W. J. Randel, and X. Zhang (1999), GSWM-98: Results for migrating solar tides, *J. Geophys. Res.*, *104*(A4), 6813–6827.

Hasebe, F. (1994), Quasi-biennial oscillations of ozone and diabatic circulation in the equatorial stratosphere, *J. Atmos. Sci.*, *51*, 729–745.

Hines, C. O. (1997a), Doppler-spread parameterization of gravity-wave momentum deposition in the middle atmosphere: 1. Basic formulation, *J. Atmos. Sol.-Terr. Phys.*, *59*, 371–386.

Hines, C. O. (1997b), Doppler-spread parameterization of gravity-wave momentum deposition in the Middle atmosphere: 2. Broad and quasi monochromatic spectra, and implementation, *J. Atmos. Sol.-Terr. Phys.*, *59*, 387.

Hollandsworth, S. M., K. P. Bowman, and R. D. McPeters (1995), Observational study of the quasi-biennial oscillation in ozone, *J. Geophys. Res.*, *100*, 7347–7361.

Huang, F. T., and C. A. Reber (2004), Non-migrating semidiurnal and diurnal tides at 95 km based on wind measurements from the High Resolution Doppler Imager on UARS, *J. Geophys. Res.*, *109*, D10110, doi:10.1029/2003JD004442.

Huang, F. T., C. A. Reber, and J. Austin (1997), Ozone diurnal variations observed by UARS and their model simulation, *J. Geophys. Res.*, *102*, 12,971–12,985.

Huang, F. T., H. G. Mayr, C. A. Reber, T. Killeen, J. Russell, M. Mlynczak, W. Skinner, and J. Mengel (2006a), Diurnal variations of temperature and winds inferred from TIMED and UARS measurements, *J. Geophys. Res.*, *111*, A10S04, doi:10.1029/2005JA011426.

Huang, F. T., H. G. Mayr, C. A. Reber, J. M Russell III, M. G. Mlynczak, and J. G. Mengel (2006b), Stratospheric and mesospheric temperature variations for the quasi-biennial and semiannual (QBO and SAO) oscillations based on measurements from SABER (TIMED) and MLS (UARS), *Ann. Geophys.*, *24*, 2131–2149.

Huang, F. T., H. G. Mayr, C. A. Reber, J. M. Russell III, M. G. Mlynczak, and J. G. Mengel (2008a), Ozone quasi-biennial oscillations (QBO), semiannual oscillations (SAO), and correlations with temperature in the mesosphere, lower thermosphere, and stratosphere, based on measurements from SABER on TIMED and MLS on UARS, *J. Geophys. Res.*, *113*, A01316, doi:10.1029/2007JA012634.

Huang, F. T., H. G. Mayr, J. M. Russell III, M. G. Mlynczak, and C. A. Reber (2008b), Ozone diurnal variations and mean profiles in the mesosphere, lower thermosphere, and stratosphere, based on measurements from SABER on TIMED, *J. Geophys. Res.*, *113*, A04307, doi:10.1029/2007JA012739.

Keckhut, P., et al. (1996), Semi-diurnal and diurnal temperature tides (30–55 km): Climatology and effect on UARS-lidar data comparisons, *J. Geophys. Res.*, *101*, 10,299–10,310.

Leblanc, T., I. S. McDermid, and D. A. Ortland (1999a), Lidar observations of the middle atmospheric thermal tides and comparison with the high-resolution Doppler Imager and Global Scale Wave Model: 1. Methodology and winter observations at table mountain (34:4°N), *J. Geophys. Res.*, *104*, 11,917–11,929.

Leblanc, T., I. S. McDermid, D. A. Ortland (1999b), Lidar observations of the middle atmospheric thermal tides and comparison with the high-resolution Doppler Imager and Global Scale Wave Model: 2. October observations at Mauna Loa (19:5°N), *J. Geophys. Res.*, *104*, 11,931–11,938.

Ling, X. D., and J. London (1986), The quasi-biennial oscillation of ozone in the tropical middle stratosphere: A one-dimensional model, *J. Atmos. Sci.*, *43*, 3122–3137.

Mayr, H. G., and J. G. Mengel (2005), Interannual variations of the diurnal tide in the mesosphere generated by the quasi-biennial oscillation, *J. Geophys. Res.*, *110*, D10111, doi:10.1029/2004JD005055.

Mayr, H. G., J. G. Mengel, K. L. Chan, and H. S. Porter (1998), Seasonal variations of the diurnal tide induced by gravity wave filtering, *Geophys. Res. Lett.*, *25*, 943–946.

McLandress, C. (1997), Seasonal variability of the diurnal tide: Results from the Canadian middle atmosphere general circulation model, *J. Geophys. Res.*, *102*, 29,747–29,767.

Mukhtarov, P., D. Pancheva, and B. Andonov (2009), Global structure and seasonal and interannual variability of the migrating diurnal tide seen in the SABER/TIMED temperatures between 20 and 120 km, *J. Geophys. Res.*, *114*, A02309, doi:10.1029/2008JA013759.

Oberheide, J., M. E. Hagan, W. E. Ward, M. Riese, and D. Offermann (2000), Modeling the diurnal tide for the Cryogenic Infrared Spectrometers and Telescopes for the Atmosphere (CRISTA) 1 time period, *J. Geophys. Res.*, *105*, 24,917–24,929.

Randel, W. J., F. Wu, R. Swinbank, J. Nash, and A. O'Neill (1999), Global QBO circulation derived from UKMO stratospheric analysis, *J. Atmos. Sci.*, *56*(4), 457–474.

Remsberg, E., G. Lingenfelser, V. Harvey, W. Grose, J. Russell III, M. Mlynczak, L. Gordley, and B. Marshall (2003), On the verification of the quality of SABER temperature, geopotential height, and wind fields by comparison with Met Office assimilated analyses, *J. Geophys. Res.*, *108*(D20), 4628, doi:10.1029/2003JD003720.

Russell, J. M., III, M. G. Mlynczak, L. L. Gordley, J. Tansock, and R. Esplin (1999), An overview of the SABER experiment and preliminary calibration results, *Proc. SPIE*, *3756*, 277–288.

Swinbank, R., R. L. Orris, and D. L. Wu (1999), Stratospheric tides and data assimilation, *J. Geophys. Res.*, *104*(DI4), 16,929–16,941.

Tian, W., M. P. Chipperfield, L. J. Gray, and J. M. Zawodny (2006), Quasibiennial oscillation and tracer distributions in a coupled chemistryclimate model, *J. Geophys. Res.*, *111*, D20301, doi:10.1029/2005JD006871.

Wu, D. L., and J. H. Jiang (2005), Interannual and seasonal variations of diurnal tide, gravity wave, ozone, and water vapor as observed by MLS during 1991–1994, *Adv. Space Res.*, *35*, 1999–2004.

Wu, D. L., C. McLandress, W. G. Read, J. W. Waters, and L. Froidevaux (1998), Equatorial diurnal variations observed in UARS microwave limb sounder temperature during 1991–1994 and simulated by the Canadian middle atmosphere model, *J. Geophys. Res.*, *103*, 8909–8917.

Xu, J., A. K. Smith, W. Yuan, H.-L. Liu, Q. Wu, M. G. Mlynczak, and J. M. Russell III (2007), Global structure and long-term variations of zonal mean temperature observed by TIMED/SABER, *J. Geophys. Res.*, *112*, D24106, doi:10.1029/2007JD008546.

Xu, J., A. K. Smith, H.-L. Liu, W. Yuan, Q. Wu, G. Jiang, M. G. Mlynczak, J. M. Russell III, and S. J. Franke (2009), Seasonal and quasi-biennial variations in the migrating diurnal tide observed by Thermosphere, Ionosphere, Mesosphere, Energetics and Dynamics (TIMED), *J. Geophys. Res.*, *114*, D13107, doi:10.1029/2008JD011298.

Yuan, T., et al. (2006), Seasonal variation of diurnal perturbations in mesopause region temperature, zonal, and meridional winds above Fort Collins, Colorado (40.6°N, 105°W), *J. Geophys. Res.*, *111*, D06103, doi:10.1029/2004JD005486.

Zawodny, J. M., and M. P. McCormick (1991), Stratospheric Aerosol and Gas Experiment II measurements of the quasi-biennial oscillations in ozone and nitrogen dioxide, *J. Geophys. Res.*, *96*, 9371–9377.

Zeng, Z., W. Randel, S. Sokolovskiy, C. Deser, Y.-H. Kuo, M. Hagan, J. Du, and W. Ward (2008), Detection of migrating diurnal tide in the tropical upper troposphere and lower stratosphere using the Challenging Minisatellite Payload radio occultation data, *J. Geophys. Res.*, *113*, D03102, doi:10.1029/2007JD008725.

Zhang, X., J. M. Forbes, M. E. Hagan, J. M. Russell III, S. E. Palo, C. J. Mertens, and M. G. Mlynczak (2006), Monthly tidal temperatures 20–120 km from TIMED/SABER, *J. Geophys. Res.*, *111*, A10S08, doi:10.1029/2005JA011504.

P. K. Bhartia, S. M. Frith, H. G. Mayr, and R. D. McPeters, NASA Goddard Space Flight Center, Greenbelt, MD 20771, USA.

F. T. Huang, Goddard Earth Sciences and Technology Center, University of Maryland, Baltimore Campus, 5523 Research Park Dr., Baltimore, MD 21228, USA. (fthuang@comcast.net)

M. G. Mlynczak, NASA Langley Research Center, Hampton, VA 23681, USA.

J. M. Russell III, Center for Atmospheric Sciences, Hampton University, Hampton, VA 23668, USA.